

Feature Article

Spectral Insights into Microdynamics of Thermoresponsive Polymers from the Perspective of Two-dimensional Correlation Spectroscopy*

Sheng-tong Sun^{a**} and Pei-yi Wu^{b**}

^a State Key Laboratory for Modification of Chemical Fibers and Polymer Materials, College of Chemistry, Chemical Engineering and Biotechnology, Center for Advanced Low-Dimension Materials, Donghua University, Shanghai 201620, China

^b State Key Laboratory of Molecular Engineering of Polymers, Collaborative Innovation Center of Polymers and Polymer Composite Materials, Department of Macromolecular Science and Laboratory for Advanced Materials, Fudan University, Shanghai 200433, China

Abstract Generalized two-dimensional correlation spectroscopy (2DCOS) and its derivate technique, perturbation correlation moving window (PCMW), have found great potential in studying a series of physico-chemical phenomena in stimuli-responsive polymeric systems. By spreading peaks along a second dimension, 2DCOS can significantly enhance spectral resolution and discern the sequence of group dynamics applicable to various external perturbation-induced spectroscopic changes, especially in infrared (IR), near-infrared (NIR) and Raman spectroscopy. On the basis of 2DCOS synchronous power spectra changing, PCMW proves to be a powerful tool to monitor complicated spectral variations and to find transition points and ranges. This article reviews the recent work of our research group in the application of 2DCOS and PCMW in thermoresponsive polymers, mainly focused on liquid crystalline polymers and lower critical solution temperature (LCST)-type polymers. Details of group motions and chain conformational changes upon temperature perturbation can thus be elucidated at the molecular level, which contribute to the understanding of their phase transition nature.

Keywords Thermoresponsive polymers; Phase transition; Two-dimensional correlation spectroscopy; Perturbation correlation moving window

INTRODUCTION

Two-dimensional correlation spectroscopy was first proposed by Noda in 1986 by detecting relatively slow relaxation processes showing sinusoidally varying spectral changes^[1]. To make this method a versatile and popular tool, later in 1993 Noda put forward the concept of generalized two-dimensional correlation spectroscopy (2DCOS) to analyze a set of spectral data upon nearly any kinds of perturbations (temperature, time, pressure, concentration, and so on)^[2]. By spreading peaks along a second dimension, 2DCOS can sort out complex and overlapped spectral features to get significantly enhanced spectral resolution. Owing to the different responses of different species to external perturbation, 2DCOS can discern the sequential order of spectral intensity changes, which is also the most recognized utility for researchers to investigate and understand

* This work was financially supported by the National Natural Science Foundation of China (Nos. 21274030, 51473038 and 21604024), the Natural Science Foundation of Shanghai (No. 17ZR1440400) and the Open Project of State Key Laboratory of Chemical Engineering (No. SKL-ChE-16C02), and “Chenguang Plan”.

** Corresponding authors: Sheng-tong Sun (孙胜童), E-mail: shengtongsun@gmail.com
Pei-yi Wu (武培怡), E-mail: peiyiwu@fudan.edu.cn

Received December 16, 2016; Revised February 9, 2017; Accepted February 17, 2017
doi: 10.1007/s10118-017-1938-1

the mechanistic insights of complex processes monitored by a spectroscopic probe.

The acquisition of 2DCOS spectra is presented in Fig. 1. A chemical system of interest is investigated by some kinds of incident electromagnetic probes such as IR, NIR and Raman. The interaction between the probes and the chemical groups in the system is recorded as a spectrum. Then additional perturbations, such as temperature and time, are applied to the system to generate a series of perturbation-dependent spectra which we often refer to as dynamic spectra. Such dynamic spectra are usually collected in a systematic manner, *e.g.* in an increment of temperature with a constant interval. Those dynamic spectra containing the information of both individual spectrum and perturbation-induced changes are subsequently subjected to a cross correlation analysis to be transformed into 2D correlation spectra^[3].

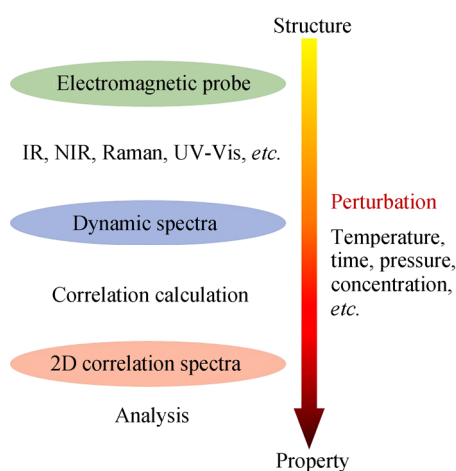


Fig. 1 Acquisition of generalized 2D correlation spectra

Up to now, 2DCOS has been proven to be a very universal and robust tool to investigate various physico-chemical phenomena at the molecular level. The broad applications of 2DCOS range from studies of basic small molecules, reactions, and composites to the characterization of polymers and biomolecules^[4]. Several reviews on the application of 2DCOS in specific fields such as hydrogen-bonding in basic molecules^[5], surface and interfacial analysis^[6], food research^[7], and protein structure and dynamics^[8] have been published. Stimuli-responsive or intelligent polymers that could respond to certain environmental stimuli such as temperature, pressure, electric field, photo-radiation or addition of small molecules, have received continuous attention over the past 30 years in both fundamental and applied research^[9]. Among them, thermoresponsive polymers are most extensively studied due to their unique temperature-responsiveness^[10]. In this article, we mainly discuss our recent work on the microdynamic studies of thermoresponsive polymers with the tools of 2DCOS and its derivative technique, perturbation correlation moving window (PCMW). The fundamental theories of 2DCOS and PCMW will be presented as well as future developments envisioned.

GENERALIZED TWO-DIMENSIONAL CORRELATION SPECTROSCOPY

The basic theory of 2DCOS will not be discussed in this paper, which has been clearly described in Noda and Ozaki's earlier papers^[2, 3, 11]. Here we only describe the principles of 2DCOS and how we read and analyze the 2DCOS spectra. Figure 2 shows the generation of 2DCOS synchronous and asynchronous spectra from a series of perturbation-dependent dynamic spectra. Three heavily overlapped simulated peaks (Figs. 2a and 2b) changing in different directions and at different rates (Fig. 2c, $A \rightarrow C \rightarrow B$, \rightarrow means prior to or earlier than) are chosen for example^[12]. As shown in Fig. 2(d), synchronous spectrum is symmetric with respect to the diagonal line, and consists of autopeaks along the diagonal line and cross-peaks located at the off-diagonal positions. The autopeaks are always positive, corresponding to the linear evolution of a certain species along the induced

perturbation, whose magnitude reflects the sensitivity of corresponding species. That is, spectral bands having higher susceptibility of intensity changes to the perturbation tend to have higher autopeak intensities. The slice trace of a synchronous spectrum along the diagonal line is called power spectrum.

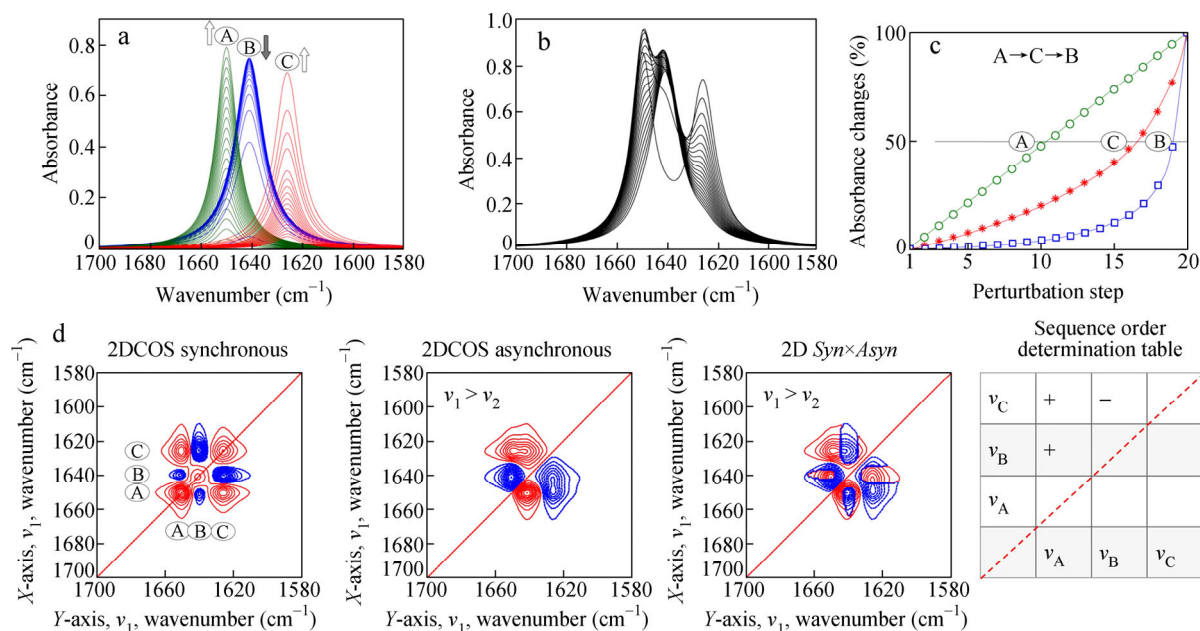


Fig. 2 (a) Simulated three heavily overlapped peaks changing in different directions and at different rates along the perturbation; (b) Overlapped 1D spectra being subject to 2D correlation analysis; (c) Normalized absorbance changes showing the sequence of variations for the three bands (A→C→B); (d) 2DCOS synchronous, asynchronous and $Syn \times Asyn$ spectra based on the three overlapped bands as well as the sequence order determination table (Red solid lines represent positive intensities, while blue dotted lines represent negative ones.) (Reprinted from Ref. [12], Copyright (2006), with permission from Elsevier)

Synchronous cross-peaks have either positive or negative signs, reflecting the relationship of spectral changes at two given wavenumbers (“+” means changes in the same direction; “-” means in the opposite direction). For example, the peaks A and C in Fig. 2 have the spectral intensities increasing while the peak B decreasing, thus showing positive cross-peaks for (A, C) and negative cross-peaks for (A, B) and (B, C) in synchronous spectrum (Fig. 2d).

Asynchronous spectrum is anti-symmetric with respect to the diagonal line, indicating sequential or unsynchronized changes of spectral intensities measured at two given wavenumbers. This correlation spectrum consists of only cross-peaks located at the off-diagonal positions. An asynchronous correlation peak can develop only if the intensities of two dynamic spectral intensities vary at different relative rates. This feature is particularly useful for 2DCOS to enhance apparent spectral resolution, even if two overlapped peaks are located very close to each other. For example, the three heavily overlapped peaks in Fig. 2 can be clearly distinguished by asynchronous spectrum (Fig. 2d).

Furthermore, the signs of cross-peaks in synchronous and asynchronous spectra can provide very useful information about the temporal sequence of events taking place during the studied process. Generally, the judging rule can be summarized as Noda’s rule—that is, if the cross-peaks (ν_1 , ν_2 , and assume $\nu_1 > \nu_2$) in synchronous and asynchronous spectra have the same sign, the change at ν_1 may occur prior to that of ν_2 , and vice versa. This rule can be simply depicted in the multiplication of synchronous and asynchronous spectra ($Syn \times Asyn$) as shown in Fig. 2(d). According to Noda’s rule, the sequential order of the three peaks in Fig. 2 can be determined to be A→C→B, which is well consistent with the result from the intensity-perturbation plot in

Fig. 2(c). It should also be noted that to deduce the sequential order by Noda's rule (one-by-one comparison by the signs of cross-peaks) is usually time-consuming and thus poorly efficient, especially for a system with more than ten peaks. Thus we proposed a simplified method through a sequence order determination table like the one shown in Fig. 2(d)^[13, 14].

PERTURBATION CORRELATION MOVING WINDOW

The interpretation of 2DCOS spectra obtained from a large data set often becomes difficult due to complicated spectral intensity variations. To simplify the spectral analysis, moving window technique was proposed by Thomas and Richardson in 2000, which is based on dynamic changes of the 2DCOS power spectrum in a small window of a subdivided data matrix moving along the perturbation direction^[15]. Later in 2006 Morita *et al.* improved this technique to much wider applicability through introducing the perturbation variable into the correlation equation, now known as perturbation correlation moving window (PCMW)^[16]. While in conventional moving window technique, only one spectrum (identical to the PCMW synchronous spectrum but with only positive signs) can be generated, in PCMW, similar to 2DCOS, a pair of synchronous and asynchronous spectra with both positive and negative signs is provided. PCMW is superior to conventional moving window by reflecting more information of spectral changes; PCMW synchronous spectrum is able to describe the changing direction of spectral intensity, and PCMW asynchronous spectrum reflects more detailed spectral variations proportional to the opposite sign of a perturbation second derivative.

PCMW can monitor very complicated spectral variations along the perturbation direction. As summarized in Fig. 3, the rules of PCMW (in the case of linear increment perturbation) are as follows: positive synchronous correlation represents spectral intensity increasing, while negative one represents decreasing; positive asynchronous correlation can be observed for a convex spectral intensity variation while negative one can be observed for a concave variation^[16].

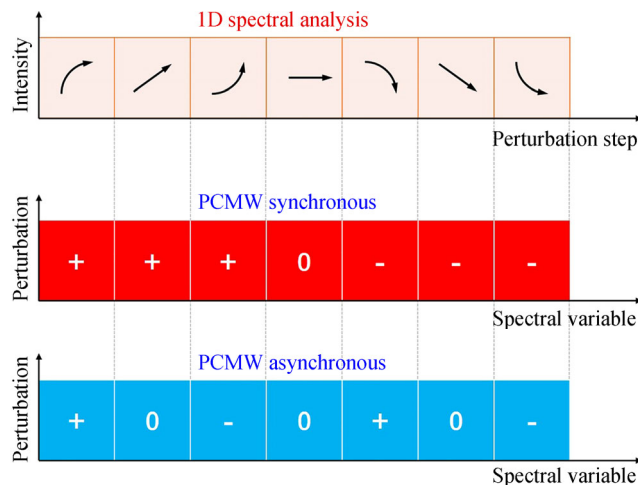


Fig. 3 Rules of PCMW (in the case of linear increment perturbation)

In practical systems, the spectral changes are often a combination of monotonic changes shown in the table. Virtually, PCMW can be applied to any kinds of perturbation-induced variations, although sometimes it is not very necessary for the systems with very simple changes. For phase transition systems which usually show sigmoidal spectral intensity variations, PCMW is rather helpful to find the transition points (peaks in synchronous spectrum) and additionally to find the transition ranges (two peaks in asynchronous spectrum corresponding to the turning points in intensity-perturbation plot). The values of transition points often imply the rough sequence of different chemical species involved under the common perturbation, which in principle should

accord with 2DCOS results. Moreover, the determination of phase transition ranges serves as an important basis for the proper selection of observation interval for 2DCOS analysis^[17].

LIQUID CRYSTALLINE POLYMERS

Liquid crystalline polymers (LCPs) are one important class of stimuli-responsive polymers widely studied in recent years. Combining properties of high molecular mass and liquid crystalline phase, LCPs have been well-known for their excellent anisotropic physical properties, easy processing and convenient molecular tailoring. Due to the rapid response of mesogens, side-chain LCP is one of the earliest studied objects by 2DCOS. Early in 1997 and 1998, Czarnecki *et al.* had employed 2D IR to study the segmental mobility of side-chain LCPs in an electric field^[18, 19].

Our group mainly focused on a novel type of LCPs, *i.e.* mesogen-jacketed liquid crystalline polymers (MJLCPs). Differing from well-known side-chain LCPs, MJLCP possesses mesogens laterally attached to the main chain with a covalent bond or a short spacer instead of long flexible decoupling spacers according to Finkelmann-Ringsdorf theory^[20]. As for a representative conventional MJCLP with rigid side groups, poly{2,5-bis[(4-methoxyphenyl)oxycarbonyl]styrene} (PMPCS), according to our 2DCOS results, it is found that before and after amorphous-to-nematic phase transition, PMPCS has a continuous motion transfer between backbone and side groups, as shown in Fig. 4^[21]. Blending 2.0 wt% graphene oxide with PMPCS does not apparently change the columnar nematic phase and sequence order of group motions, while due to the presence of π - π stacking interactions and charge transfer between PMPCS and GO sheets, a two-step mesophase transition process defined as a physical adsorption process and a mesophase development process under physical cross-linking can be identified by 2DCOS^[22].

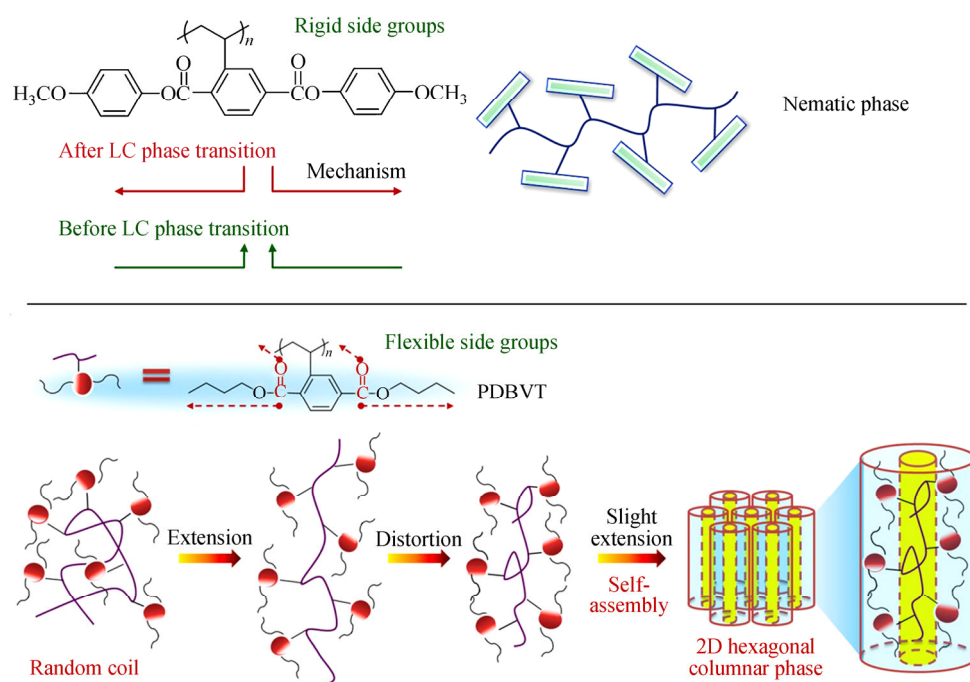


Fig. 4 Top: chemical structure of PMPCS and schematic illustration of the sequence of group motions before and after LC phase transition; Bottom: the sequence of group motions and schematic self-assembly process of 2D hexagonal columnar phase formation of PDBVT on mesoscale during heating (The blue and yellow colors represent different electron densities.) (Reproduced with permission from Ref. [14]; Copyright (2009) American Chemical Society; Reproduced with permission from Ref. [21]; Copyright (2005) American Chemical Society)

If the mesogenic side groups of MJLCs are replaced by flexible alkyl chains, novel LCs which exhibit unexpected thermotropic liquid crystallinity without conventional mesogens can be obtained. We further employed IR in combination with 2DCOS to study the precise supramolecular self-assembly nature of poly[di(butyl)vinylterephthalate] (PDBVT, structure as shown in Fig. 4), which can self-assemble into two-dimensional hexagonal columnar ($2D \Phi_H$) phase without conventional mesogens^[14]. 2DCOS results conclusively showed that carbonyl groups act as the starting point of molecular motions upon heating, and have a significant influence on the formation of $2D \Phi_H$ phase; PDBVT backbones experience “extension-distortion-slight extension” consecutive motions, as illustrated in Fig. 4. This mechanism is largely different from that of PMPCS. Later we also reported further interpretation of the role of carbonyl groups on the columnar phase formation of PDBVT^[23] and detailed conformational changes of the aliphatic side groups during LC phase development^[24].

In the case of PDBVT, PCMW also showed its powerfulness in determining the phase transition points and transition temperature ranges. As stated earlier, the phase transition systems such as PDBVT and PCMW often show one point in synchronous spectrum and two turning points in asynchronous spectrum, which correspond to the transition temperature and transition temperature range, respectively. As shown in Fig. 5, different peaks in PCMW synchronous spectrum show consistent LC transition temperature of $\sim 90^\circ\text{C}$, in accordance with Boltzmann fitting results based on conventional IR analysis. More importantly, PCMW asynchronous spectrum additionally determines the LC transition temperature range to be $70\text{--}110^\circ\text{C}$, corresponding to the two turning points in the ‘anti-S’ shaped Absorbance-Temperature curves^[14]. In view of the whole spectral analysis, PCMW is quite reliable and much more superior to conventional IR analysis.

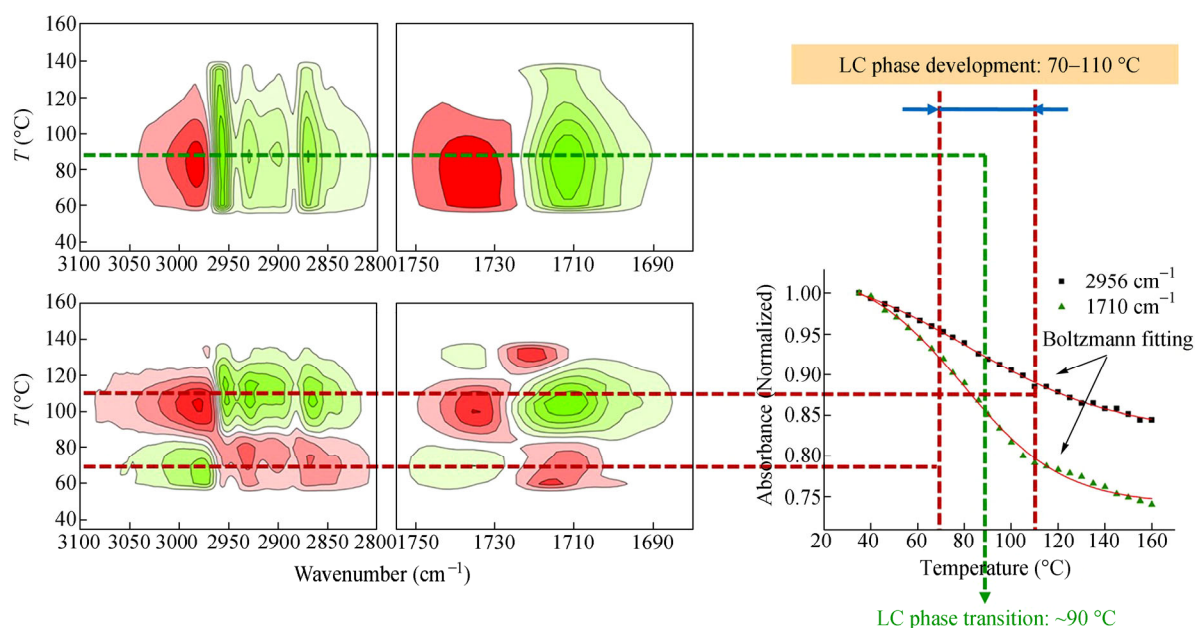


Fig. 5 PCMW synchronous and asynchronous spectra and Boltzmann fitting results based on conventional IR analysis for the LC phase transition of PDBVT during heating (red, positive; green, negative) (Reproduced with permission from Ref. [14]; Copyright (2009) American Chemical Society)

LCST-TYPE WATER-SOLUBLE POLYMERS

LCST-type polymers (LCST, lower critical solution temperature) are mostly studied thermoresponsive polymers due to their unique temperature-sensitive nature in water, *i.e.* an abrupt and reversible phase separation as the ambient temperature exceeds LCST. Comprehension of the phase transition behavior of LCST-type polymers

can help us understand the nature of some life phenomenon such as protein denaturation. Poly(*N*-isopropylacrylamide) (PNIPAM) is the most representative LCST-type polymer with LCST around 32 °C, very close to physiological temperature. Upon heating to its LCST, the PNIPAM aqueous solution undergoes a coil-to-globule phase transition and can recover easily its original state upon cooling^[25]. Besides PNIPAM, a wide range of other LCST-type polymers have also been reported to demonstrate similar trend for smart materials, such as poly(*N*-vinylcaprolactam) (PVCL), poly(vinyl methyl ether) (PVME), poly(2-isopropyl-2-oxazoline) (PIPOZ), oligo(ethylene glycol) methacrylate-based polymer (POEGMA), and some poly(ionic liquid)s (PILs)^[10]. By 2DCOS and PCMW, in recent years our group studied the microdynamic mechanisms of a series of LCST-type polymers in various forms like homopolymers, random copolymers, block copolymers, mixtures, hydrogels and microgels. Here we use some examples to present our recent progress in this topic.

LCST-type Linear Polymers

We used to study the typical reversible phase transitions of PNIPAM in aqueous solutions. The transition of PNIPAM is generally considered to be the competitive result of the hydrophobic interaction of pendent isopropyl groups and backbones and the hydrogen bonding association between amide groups and water molecules. From 2DCOS analysis, we found that as temperature rises a two-step dehydration of methyl groups occurs first, then the main-chain diffusion and aggregation take place followed by the hydrogen bond transition, while the sequence in the cooling process is just the opposite^[26]. PCMW and 2DCOS were also employed to study the phase transition behavior of PNIPAM as well as its small molecular model compound *N*-isopropylpropionamide (NIPPA)^[27]. The presence of main chains does not affect the sensitivity and changing sequence of different groups, but has a strong effect on the size of aggregation and formation of hydrogen bonds between carbonyl groups and water molecules. Moreover, the roles of methanol and ionic liquids due to strong additive-water association dynamics on the thermosensitivity of PNIPAM in water were also investigated^[28, 29].

POEGMA is another important class of LCST-type polymers, whose transition temperature can be precisely adjusted using a simple random copolymerization of OEG macromonomers of different chain lengths *n* (*i.e.*, of different hydrophilicity but similar chemical nature) by living polymerization methods. We studied the dynamic thermally reversible hydration behavior of a well-defined thermoresponsive copolymer P(MEO₂MA-*co*-OEGMA₄₇₅) in D₂O synthesized by ATRP random copolymerization of 2-(2-methoxyethoxy)ethyl methacrylate (MEO₂MA) and oligo(ethylene glycol) methacrylate (*M_n* = 475 g/mol) by means of IR spectroscopy in combination with PCMW and 2DCOS^[30]. Largely different from PNIPAM, P(MEO₂MA-*co*-OEGMA₄₇₅) exhibits a sharp change below LCST and a gradual change above LCST due to the absence of strong intermolecular hydrogen bonding interactions between polymer chains, and the apparent phase transition is mainly arising from the multiple chain aggregation without a precontraction process of individual polymer chains. PCMW determined the phase transition temperature to be *ca.* 32.5 °C during heating and *ca.* 31 °C during cooling as well as the transition temperature range to be 28.5–37 °C. During phase transition, P(MEO₂MA-*co*-OEGMA₄₇₅) chains successively experience “hydrated chains-dehydrated chains-loosely aggregated micelles-densely aggregated micelles” four consecutive conformation changes, as shown in Fig. 6. When the chain of one monomer, oligo(ethylene glycol) methacrylate, becomes longer, P(MEO₂MA-*co*-OEGMA₁₀₈₀) exhibits an unusual thermally induced multistep aggregation process^[31].

Except PNIPAM and POEGMA, the microdynamic mechanisms of several other LCST-type linear polymers such as PVME^[32–34], PVCL^[35], PIPOZ^[36], PIL^[37, 38], and poly(3-ethyl-*N*-vinyl-2-pyrrolidone) (C2PVP)^[39] were also investigated by our group, which show distinct phase transition behavior due to different chemical structures.

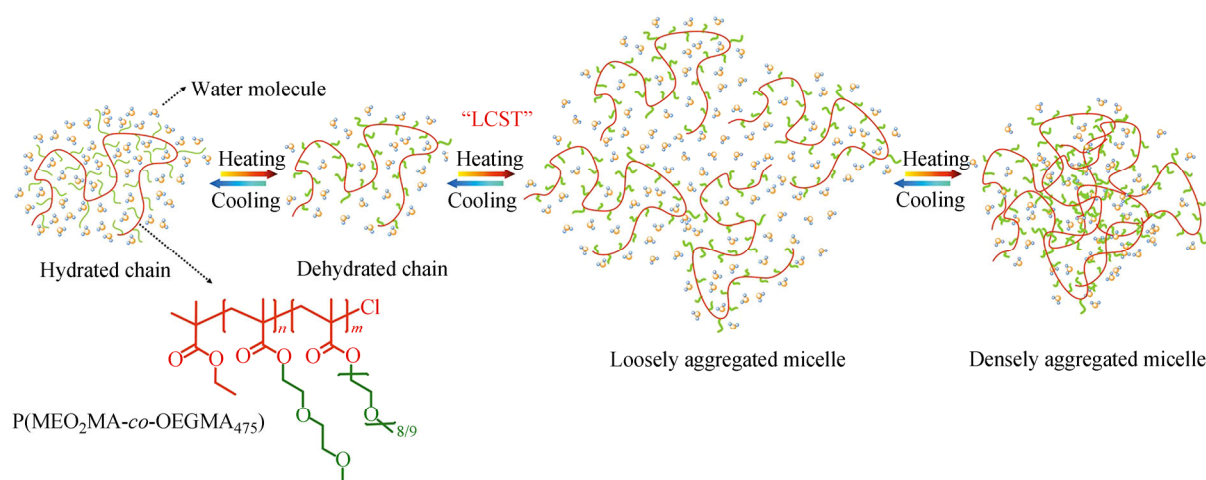


Fig. 6 Schematic conformational changes of P(MEO₂MA-co-OEGMA₄₇₅) chains during phase transition (Reproduced with permission from Ref. [30]; Copyright (2013) American Chemical Society)

LCST-type Block Copolymers and Mixtures

Block copolymers composed of thermoresponsive blocks are of great interest due to their distinct self-assembly behavior in case of different linking architectures or different stimuli applied. In our group, thermoresponsive block copolymers with either linear or nonlinear architectures have been investigated by the tools of 2DCOS and PCMW.

For example, we employed IR spectroscopy in combination with 2DCOS and PCMW to elucidate the dynamic self-aggregation behavior of a novel miktoarm star PNIPAM-based multihydrophilic block copolymer, poly(*N*-isopropylacrylamide)₂-[poly(*N*-vinylpyrrolidone)-*b*-poly(acrylic acid)]₂ ((PNIPAM)₂-(PVP-*b*-PAA)₂) (chemical structure as shown in Fig. 7a)^[40]. At pH = 8, (PNIPAM)₂-(PVP-*b*-PAA)₂ tends to self-assemble into micelles with PNIPAM in the core and ionized PAA segments in the shell during heating. As shown in Fig. 7(b), as temperature increases, all the C–H stretching bands shift to lower frequency due to a gradual strengthening of hydrophobic interaction of polymer chains. PAA segments are only partially ionized showing C=O stretching vibrations from both COOD and COO[−] groups. The binary spectral intensity change of amide I groups in PNIPAM segments is attributed to the transformation of hydrogen bonded C=O with water to self-associated ones, which is characteristic for PNIPAM-related LCST-type phase transition^[26, 28]. PCMW synchronous and asynchronous spectra show the transition temperature and transition temperature range respectively, as presented in Fig. 7(c). However, due to the different response of different chemical species, the transition temperatures obtained from different origins usually differ from each other. From the transition temperature region plot, we can roughly conclude that PNIPAM segments have an earlier response than PAA segments. Consistently, later 2DCOS analysis discerns a sequential group motion from PNIPAM to PVP and PAA segments. It is finally concluded that the three polymeric segments have relatively independent phase behavior during the formation of PNIPAM-core micelles, and the chain conformation induced by hydrophilic-to-hydrophobic transformation of PNIPAM segments should be the driving force of the whole self-aggregation process. The proposed self-aggregation mechanism of (PNIPAM)₂-(PVP-*b*-PAA)₂ in D₂O during heating is shown in Fig. 7(d).

Additionally, we also investigated the thermal-induced self-assembly behavior of other LCST-type block copolymers such as diblock copolymers, poly(NIPAM-*b*-BVIImBr)^[41], PNIPAM-*b*-PEO^[42], POEGMA-*b*-P4VP^[43] and PVCL-*b*-PEO^[44], or triblock copolymers, PEO-*b*-PPO-*b*-PEO^[45], and PDEGA-*b*-PDMA-*b*-PVCL^[46].

It is also interesting to investigate the interactions between two different LCST-type polymers when mixed together. For instance, we employed IR and 2DCOS to compare the phase transition behaviors of PIPOZ/PNIPAM and PNIPAM/PVCL mixtures, as depicted in Fig. 8^[47]. Through comparison, we found that

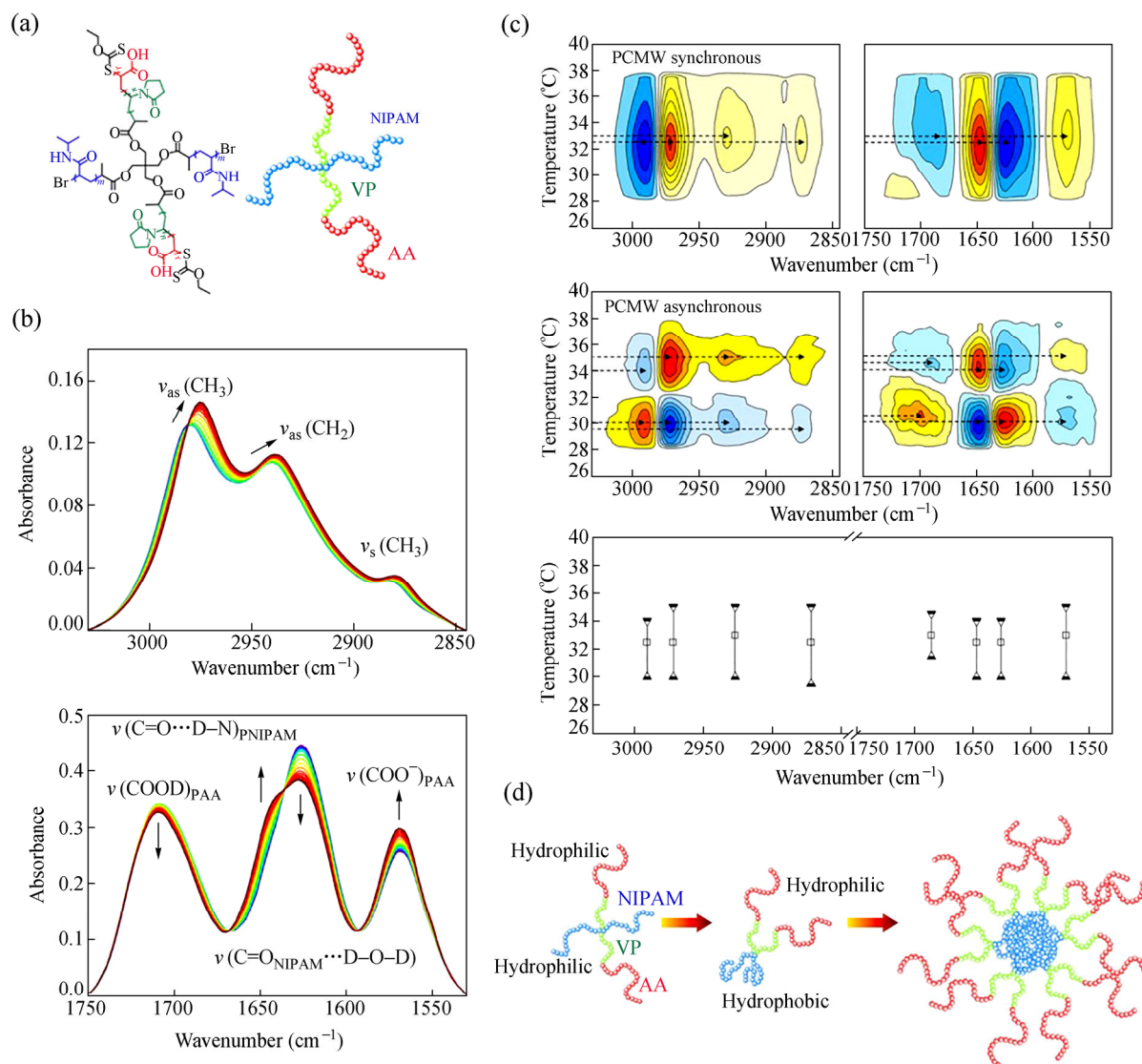


Fig. 7 (a) Chemical structure of (PNIPAM)₂-(PVP-*b*-PAA)₂ and its corresponding schematic illustration (Wherein, $m = 47$, $n = 38$, $r = 45$); (b) Temperature-dependent FTIR spectra of (PNIPAM)₂-(PVP-*b*-PAA)₂ in D₂O (10 wt%) at pH = 8 during heating between 26 and 40 °C in the regions 3030–2845 cm⁻¹ and 1750–1530 cm⁻¹; (c) PCMW synchronous and asynchronous spectra as well as corresponding transition temperature region plot (red and yellow, positive; blue, negative); (d) Schematic illustration of dynamic self-aggregation behavior of (PNIPAM)₂-(PVP-*b*-PAA)₂ in D₂O during heating (Reproduced with permission from Ref. [40])

PVCL chains can interact with PIPOZ chains directly through the polymer-water-polymer cross-linking hydrogen bonds ($C=O \cdots D-O-D \cdots O=C$), which induce their transition process as one. However, in the PIPOZ/PNIPAM mixture, the phase transition of the given component (PNIPAM or PIPOZ) is indirectly affected by the presence of the second component, because the strong hydrogen bonds $C=O \cdots D-N$ in PNIPAM components forbid the direct connection with PIPOZ, which induces two phase transition processes separately with no liquid-liquid phase separation (LLPS). However, in the case of the mixture of PNIPAM and a thermoresponsive PIL, P[P_{4,4,4,4}][SS], the phase transition behavior of P[P_{4,4,4,4}][SS] is largely suppressed^[48]. Similarly, we also studied the phase transition behaviour of the mixture of a thermoresponsive ionic liquid, [P_{4,4,4,6}][MC3S], and another LCST-type polymer, PNIPAM or PVCL^[49].

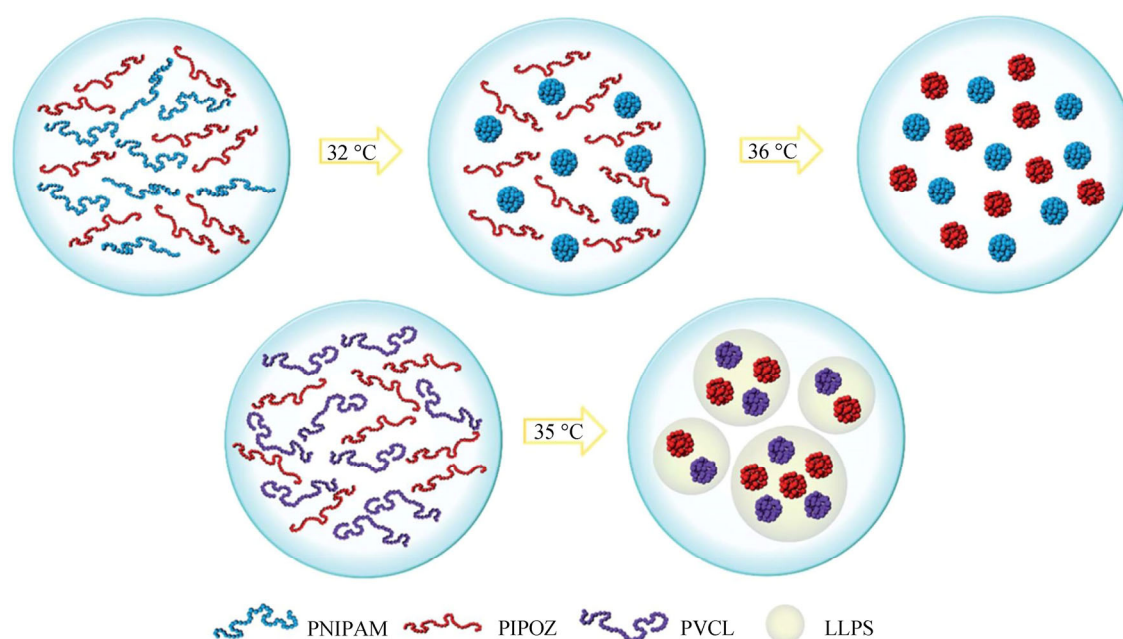


Fig. 8 Schematic illustration of the dynamic changing process of PIPOZ/PNIPAM mixture (top) and PIPOZ/PVCL mixture (bottom) solutions during heating (Reproduced with permission from Ref. [47])

LCST-type Hydrogels and Microgels (or Nanogels)

Hydrogels are crosslinked polymer networks capable of absorbing large quantities of water, and microgels or nanogels are nanosized hydrogels. Specially, owing to the temperature-dependent volume phase transition (VPT), LCST-type hydrogels and nanogels are promising for a variety of applications such as drug delivery, catalysis, sensor, *etc*^[50]. We are also interested in the microdynamic mechanism of LCST-type hydrogels/nanogels which are largely different from LCST-type polymers in aqueous solutions due to the presence of crosslinking network.

For example, we employed IR with 2DCOS and PCMW to study the chain collapse and revival processes of PNIPAM hydrogel upon a heating-cooling cycle, and we found that the chain collapse of PNIPAM hydrogel takes place along with some intermediate states or a completely continuous phase transition while the chain revival occurs with only conversion between two single states. In the heating process, PNIPAM hydrogel occurs to collapse along the backbone before water molecules are expelled outside the network, while in the sequential cooling process, PNIPAM hydrogel has water molecules diffusing into the network first before the chain revival along the backbone occurs^[51]. Introduction of a comonomer of acrylic acid (AA) to this hydrogel leads to the irreversible recovery of PNIPAM-*co*-AA hydrogel during cooling^[52].

Nevertheless, the rapid water diffusion process can be ignored in the volume phase transition of nanogels with a largely reduced size. As shown in Fig. 9, we studied the volume phase transition behavior of well-defined thermoresponsive poly(2-methoxyethyl acrylate-*co*-poly(ethylene glycol) methyl ether acrylate)/poly(*N,N'*-dimethylacrylamide) (P(MEA-*co*-PEGA)/PDMA) and PNIPAM/poly(*N,N'*-dimethylacrylamide) (PNIPAM/PDMA) core-shell nanogels^[53]. It is found that the continuous dehydration of the C=O groups in the P(MEA-*co*-PEGA)/PDMA nanogel core predominates the linear volume phase transition while the hydrogen bonding transformation in the PNIPAM/PDMA nanogel core leads to the abrupt decrease in nanogel size on heating. Additionally, considering the core and the shell separately, for both nanogels, the inner core contributes much more to the volume phase transition and the outer shell only undergoes slight dehydration following the core on heating.

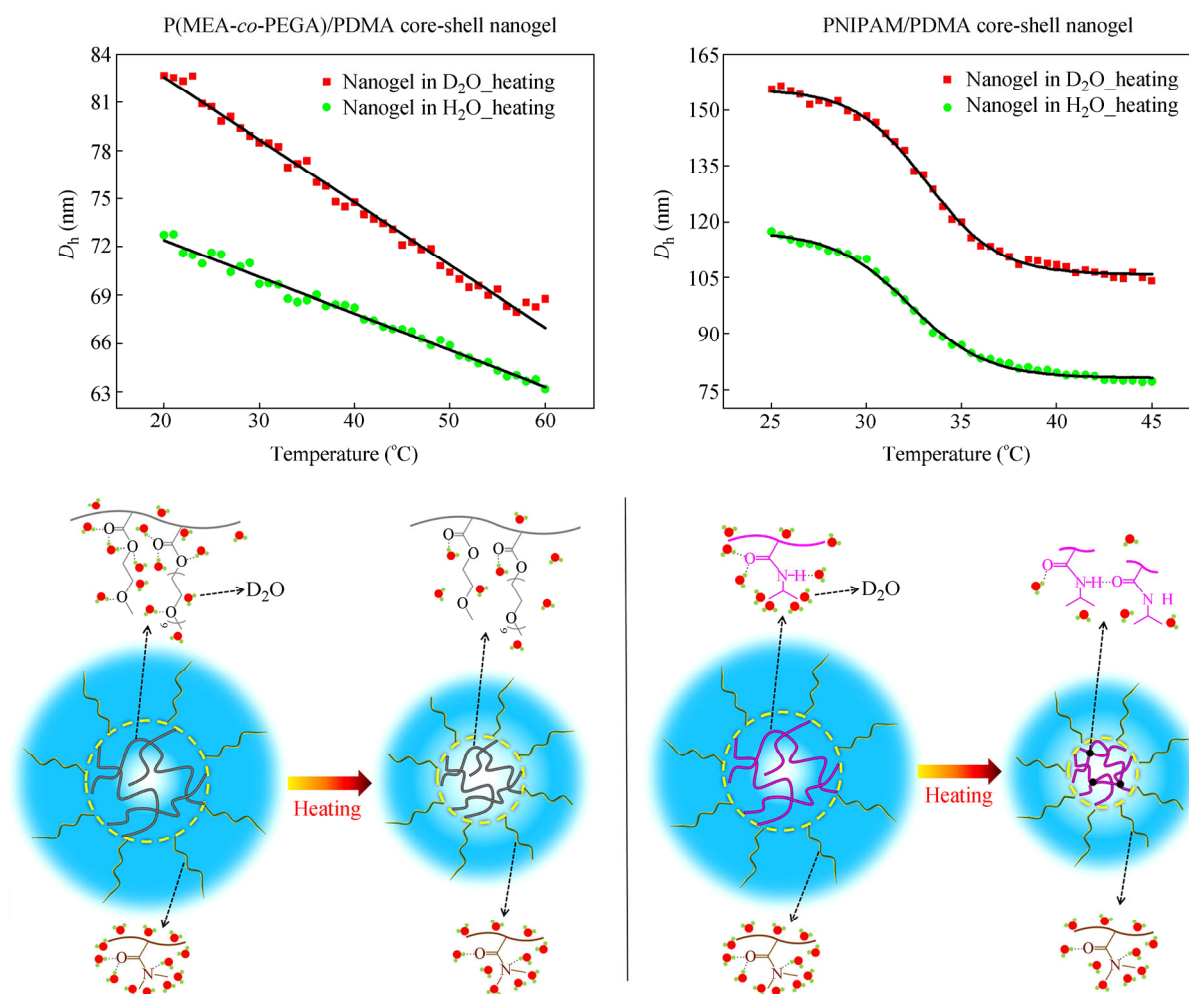


Fig. 9 Schematic illustration of the volume phase transition mechanisms of P(MEA-co-PEGA)/PDMA and PNIPAM/PDMA core-shell structured nanogels (Reproduced with permission from Ref. [53]; Copyright (2014) American Chemical Society)

Besides, by means of 2DCOS and PCMW, we also studied the volume phase transition behavior of PNIPAM/PHEMA (poly(2-hydroxyethyl methacrylate)) interpenetrating microgels^[54], POEGMA microgels with PIL cross-linkers^[55], as well as gold nanoparticle- or carbon nanodot-incorporated PVCL microgels^[56, 57].

CONCLUSIONS AND OUTLOOK

2DCOS has gained great progress both in experimental and theoretical methodologies in the past decade, and proves to be a very robust and powerful analytical tool in studying diverse polymeric systems. As a 2DCOS-derivative technique, PCMW is particularly helpful to simplify complicated spectral variations and to find transition points and ranges, especially for phase transition systems as reviewed in this article. Owing to the features of spectral resolution enhancement and sequence order discernment, according to our work, 2DCOS as well as PCMW has clearly shown their powerfulness in understanding the mechanistic insights of the microdynamics of thermoresponsive polymers. In view of the rapid development of new thermoresponsive polymeric systems with different components and forms like brushes, micelles, capsules, composite hydrogels, membranes, *etc.*^[9, 10], we can easily foresee the future wide applications of 2DCOS and PCMW in this area in case proper dynamic spectra can be obtained. We also hope that our 2DCOS research on thermoresponsive polymers may enlighten more scientists from different disciplines engaged in this interesting field.

Furthermore, for 2DCOS beginners, it is worth noting that in practical applications with complicated spectral variations, it needs to be paid careful attention to perform 2DCOS analysis in a properly selected data set with monotonic spectral changes to obtain reliable results. It is strongly recommended to plot and examine intensity versus perturbation curves before performing 2DCOS analysis. PCMW-based segmental analysis is also an alternative method. Also, it needs to be noticed that the interpretation of 2DCOS results should be closely associated with other characterization results for a specific system, which should be consistent with each other.

REFERENCES

- 1 Noda, I., *Bull. Am. Phys. Soc.*, 1986, 31: 520
- 2 Noda, I., *Appl. Spectrosc.*, 1993, 47(9): 1329
- 3 Noda, I. and Ozaki, Y., "Two-dimensional correlation spectroscopy: Applications in vibrational and optical spectroscopy", Chichester: Wiley, 2004
- 4 Park, Y., Noda, I. and Jung, Y.M., *J. Mol. Struct.*, 2016, 1124: 11
- 5 Czarnecki, M.A., *Appl. Spectrosc. Rev.*, 2011, 46(1): 67
- 6 Dluhy, R., Shanmukh, S. and Morita, S.I., *Surf. Interface Anal.*, 2006, 38(11): 1481
- 7 You, Z., Zhuo, L., Yang, X., Hong, H., Liu, Z., Gong, Z. and Cheng, F., *Appl. Spectrosc. Rev.*, 2015, 50(10): 840
- 8 Shashilov, V.A. and Lednev, I.K., *J. Raman Spectrosc.*, 2009, 40(12): 1749
- 9 Stuart, M.A.C., Huck, W.T.S., Genzer, J., Muller, M., Ober, C., Stamm, M., Sukhorukov, G.B., Szleifer, I., Tsukruk, V.V., Urban, M., Winnik, F., Zauscher, S., Luzinov, I. and Minko, S., *Nat. Mater.*, 2010, 9(2): 101
- 10 Roy, D., Brooks, W.L.A. and Sumerlin, B.S., *Chem. Soc. Rev.*, 2013, 42(17): 7214
- 11 Morita, S., Shinzawa, H., Tsenkova, R., Noda, I. and Ozaki, Y., *J. Mol. Struct.*, 2006, 799(1): 111
- 12 Czarnik-Matusewicz, B., Pilorz, S., Ashton, L. and Blanch, E.W., *J. Mol. Struct.*, 2006, 799(1-3): 253
- 13 Sun, S., Tang, H. and Wu, P., *Phys. Chem. Chem. Phys.*, 2009, 11(35): 7611
- 14 Sun, S.T., Tang, H., Wu, P.Y. and Wan, X.H., *Phys. Chem. Chem. Phys.*, 2009, 11(42): 9861
- 15 Thomas, M. and Richardson, H.H., *Vib. Spectrosc.*, 2000, 24(1): 137
- 16 Morita, S., Shinzawa, H., Noda, I. and Ozaki, Y., *Appl. Spectrosc.*, 2006, 60(4): 398
- 17 Wang, M.Y., Sun, S.T. and Wu, P.Y., *Appl. Spectrosc.*, 2010, 64(12): 1396
- 18 Czarnecki, M.A., Okretic, S. and Siesler, H.W., *J. Phys. Chem. B*, 1997, 101(3): 374
- 19 Czarnecki, M.A., Okretic, S. and Siesler, H.W., *Vib. Spectrosc.*, 1998, 18(1): 17
- 20 Chen, X.F., Shen, Z., Wan, X.H., Fan, X.H., Chen, E.Q., Ma, Y. and Zhou, Q.F., *Chem. Soc. Rev.*, 2010, 39(8): 3072
- 21 Shen, Y., Chen, E.Q., Ye, C., Zhang, H.L., Wu, P.Y., Noda, I. and Zhou, Q.F., *J. Phys. Chem. B*, 2005, 109(13): 6089
- 22 Jing, Y., Tang, H. and Wu, P., *Polym. Chem.*, 2013, 4(24): 5768
- 23 Sun, S.T., Tang, H. and Wu, P.Y., *J. Phys. Chem. B*, 2010, 114(10): 3439
- 24 Tang, H., Sun, S.T., Wu, J.W., Wu, P.Y. and Wan, X.H., *Polymer*, 2010, 51(23): 5482
- 25 Schild, H.G., *Prog. Polym. Sci.*, 1992, 17(2): 163
- 26 Sun, B., Lin, Y., Wu, P. and Siesler, H.W., *Macromolecules*, 2008, 41(4): 1512
- 27 Lai, H.J. and Wu, P.Y., *Polymer*, 2010, 51(6): 1404
- 28 Sun, S.T. and Wu, P.Y., *Macromolecules*, 2010, 43(22): 9501
- 29 Wang, Z.W. and Wu, P.Y., *RSC Adv.*, 2012, 2(18): 7099
- 30 Sun, S. and Wu, P., *Macromolecules*, 2013, 46(1): 236
- 31 Zhang, B., Tang, H. and Wu, P., *Macromolecules*, 2014, 47(14): 4728
- 32 Gu, W.X. and Wu, P.Y., *Anal. Sci.*, 2007, 23(7): 823
- 33 Guo, Y., Sun, B. and Wu, P., *Langmuir*, 2008, 24(10): 5521
- 34 Sun, B.J., Lai, H.J. and Wu, P.Y., *J. Phys. Chem. B*, 2011, 115(6): 1335
- 35 Sun, S. and Wu, P., *J. Phys. Chem. B*, 2011, 115(40): 11609
- 36 Li, T., Tang, H. and Wu, P., *Langmuir*, 2015, 31(24): 6870
- 37 Li, W. and Wu, P., *Polym. Chem.*, 2014, 5(19): 5578

- 38 Wang, G. and Wu, P., *Soft Matter*, 2015, 11(26): 5253
- 39 Lai, H.J., Chen, G.T., Wu, P.Y. and Li, Z.C., *Soft Matter*, 2012, 8(9): 2662
- 40 Sun, S.T., Zhang, W.D., Zhang, W., Wu, P.Y. and Zhu, X.L., *Soft Matter*, 2012, 8(14): 3980
- 41 Wang, Z., Lai, H. and Wu, P., *Soft Matter*, 2012, 8(46): 11644
- 42 Wang, Q., Tang, H. and Wu, P., *Langmuir*, 2015, 31(23): 6497
- 43 Dai, Y. and Wu, P., *Phys. Chem. Chem. Phys.*, 2016, 18(31): 21360
- 44 Wang, Q., Tang, H. and Wu, P., *J. Polym. Sci., Part B: Polym. Phys.*, 2016, 54(3): 385
- 45 Jia, L., Guo, C., Yang, L., Xiang, J., Tang, Y., Liu, C. and Liu, H., *J. Colloid Interf. Sci.*, 2010, 345(2): 332
- 46 Ye, Z., Li, Y., An, Z. and Wu, P., *Langmuir*, 2016, 32(26): 6691
- 47 Li, T., Tang, H. and Wu, P., *Soft Matter*, 2015, 11(15): 3046
- 48 Wang, G. and Wu, P., *Langmuir*, 2016, 32(15): 3728
- 49 Wang, G. and Wu, P., *Soft Matter*, 2016, 12(3): 925
- 50 Motornov, M., Roiter, Y., Tokarev, I. and Minko, S., *Prog. Polym. Sci.*, 2010, 35(1-2): 174
- 51 Sun, S., Hu, J., Tang, H. and Wu, P., *J. Phys. Chem. B*, 2010, 114(30): 9761
- 52 Sun, S., Hu, J., Tang, H. and Wu, P., *Phys. Chem. Chem. Phys.*, 2011, 13(11): 5061
- 53 Hou, L., Ma, K., An, Z. and Wu, P., *Macromolecules*, 2014, 47(3): 1144
- 54 Zhang, B., Sun, S. and Wu, P., *Soft Matter*, 2013, 9(5): 1678
- 55 Zhou, Y., Tang, H. and Wu, P., *Phys. Chem. Chem. Phys.*, 2015, 17(38): 25525
- 56 Hou, L. and Wu, P., *RSC Adv.*, 2014, 4(74): 39231
- 57 Sun, W. and Wu, P., *Phys. Chem. Chem. Phys.*, 2017, 19(1): 127